Modified Lewis Correlation for Desiccant Dehumidification Process

M. H. Gurses [1], A. Ertas [2]*

[1]Gonca OSGB, Istanbul, Turkey; e-mail: melihgurses@goncaosgb.com

[2]Department of Mechanical Engineering, Texas Tech University, Lubbock, Texas, 79409

Received 8 December, 2021; Revised 22 March, 2022; Accepted 2 April, 2022

Available online 3 April, 2022 at www.atlas-tjes.org, doi: 10.22545/2022/00172

Using effective tower design utilized in the dehumidification of air has potential applications in many fields,e.g., air-conditioning, crop-drying, meat, and fish drying, to reduce energy consumption. One of the most important parameters for packed tower design is the correct calculation of the Lewis Correlation. In this study, the Lewis Correlation method is summarized, and the agreements and disagreements are discussed. The Lewis Correlation method is modified for packed tower applications. This modification is based on the assumption that the water layer is thick and therefore the change in the interfacial temperature with tube length varies. The resulting equations are applied to water and liquid desiccants.

Keywords: Packed tower, Lewis correlation, liquid desiccant, vapor pressure equilibrium.

1 Introduction

Using effective tower design utilized in dehumidification of air has potential applications in many fields, e.g., air-conditioning, crop-drying, meat, and fish drying, to reduce energy consumption. One of the most important parameters for packed tower design is the correct calculation of the Lewis Correlation. Walker, Lewis, and McAdams [1] proposed a basic theory for cooling tower operation in 1923. Lewis [2] proposed an approximate relation for cooling water systems by assuming the interface temperature along the height of the cooling tower and Merkel [3] developed the first practical use of Lewis' relation in 1925. The Lewis relation was based on the assumption that the interface temperature is equal to the liquid temperature, and states that the ratio of the heat transfer coefficient to the coefficient of vapor diffusion through the gas film is constant and equal to the heat capacity of the humid air which can be expressed by a constant. In 1933, Lewis [4] found, through experimentation, that this ratio was greater than twice the initial estimate. Hensel and Treyball [5] determined that the interface temperature was not equal to the liquid temperature and noted that the apparent psychometric ratio for a packed tower is neither constant nor equal to the heat capacity of the humid air, as previously postulated. Lof, et al. [6] supported this result and concluded that until additional data was available, the design of packed towers should be based on a heat/mass transfer coefficient ratio of about 0.5 rather than 0.24 Btu/lb °F.

Many experiments have been performed in the past to correlate relations concerning heat and mass transfer between air and water. The air in the atmosphere contains 0%-4% water vapor. There are several applications of air-water vapor mixtures. One such application in engineering is air conditioning. Although the amount of water in the air is small, it plays a major role in human comfort. Temperature, humidity, mass transfer, dust, clearness, and sound can affect comfort. Dehumidification of air can be achieved by refrigeration, mechanical compression, or using desiccants. To condense the excess moisture, the air is cooled below the saturation temperature, compressed mechanically, or desiccants are used. Of these three operations, desiccant dehumidification has two major advantages over the other three operations. These are low drying temperatures and low cost. Desiccants are chemicals that have the ability to absorb moisture from different media. To reuse the desiccants or in other words, to evaporate the absorbed moisture from the desiccant, regeneration is necessary. The desiccant regeneration process requires the application of heat to drive off the moisture. There are two kinds of desiccants: Solid desiccants and liquid desiccants. Many chemicals can be used as liquid desiccants. e.g. lithium chloride, sodium or potassium hydroxide, mono ethylene, sulphuric acid, phosphoric acid, etc. Liquid desiccants have low vapor pressure, are nontoxic, and have the ability to be regenerated at low temperatures. Moreover, liquid desiccants clean up the air from contaminants and disinfect it. When the liquid desiccant and air are brought into contact with each other, depending on the concentration of the liquid desiccant, moisture tends to move from the gas phase to the liquid phase. The driving force in this phase change is the difference between the vapor of the liquid desiccant and the vapor pressure of the air.

In liquid desiccant systems, air and liquid desiccant can be brought into contact by flowing them through a counter flow tower such as a spray tower, a packed tower, or a wetted–wall tower. To regenerate the liquid desiccant, either the air or the desiccant is heated. A packed tower, vertical columns filled with packing or other devices to provide a large interfacial surface area, keeps the air and liquid desiccant in contact continuously. The liquid desiccant is distributed over the packing as a thin liquid film and it then flows downward under the influence of gravity. The air, which is moved upward through the wet packing by fans experiences a considerable pressure drop. Strigle [7] developed equations for the air side pressure drop related to the air velocity for counterflow towers. The pressure drop in packed towers is dependent on both the air and liquid flow rates. If the gas velocity is fixed, the gas pressure drop increases with an increased liquid flow rate. Treybal [3] discusses problems due to the large pressure drop across the packed column. The selection of packing materials is important to minimize the pressure drop and to provide maximum interface surface area.

Lof et al. [6] examined a cooling system, combined with and operated by a solar air heating process, based on the concept of an open–cycle LiCl absorption air conditioning system. A packing made from 1–inch ceramic rashing rings was utilized. The resultant heat transfer coefficient was found to be within the expected range as predicted by the correlation of McAdams et al. [8] for pure water flowing in a column packed with 1–inch rings. The difference between the measured heat transfer coefficient and the McAdams correlation was about 10 percent. However, Lof et al. [6] were not satisfied with the mass transfer coefficient found by McAdams et al. [8].

Sherwood and Holloway [9] did the first extensive investigation relating to liquid mass transfer coefficients for packed towers. They studied the desorption of carbon dioxide, oxygen, or hydrogen from water using a variety of packing materials. They used different size ceramic rasching rings and berl saddles, and found that the volumetric mass transfer is the most widely used correlation because of its simplicity and its requirement of well–documented physical properties. In 1942, Molstad et al. [10] collected data for a square tower with approximately the same cross–sectional area of the study of Sherwood and Holloway [9]. Molstad et al. [10] used Sherwood and Holleway's correlation to determine the constants. Vivian and Whitney [11] also employed a similar process to find additional data for the desorption of oxygen from water in packed columns. Vivian and Whitney's [11] results were found to agree well with those of Sherwood and Holloway [9]. Norman [12] used the same data as Sherwood and Holloway [9], and Molstad [10] for different packings and found smaller values for the volumetric mass transfer. Sherwood and Pigford [13] reported that one of the equations did not give accurate data for absorption as reported by Sherwood and Holloway [8]. Puranik and Vogelpohl [14] developed a correlation for predicting values of the effective interfacial area based on the concepts of static and dynamic area. With these three equations, all values of the interfacial area during vaporization, absorption with and without chemical reaction, and wetted surface area can be predicted within a range of ± 20 percent accuracy. However, many investigators concluded that further investigations are necessary for the contact of air and liquid at the interface.

Because of the difficulty of measurements, the interfacial temperature is usually assumed to be equal to the bulk temperature of the liquid. In 1922, Lewis [2] established an important relationship for calculating the humidity of air from wet– and dry–bulb thermometer readings and showed that the ratio of the heat transfer coefficient to the diffusion coefficient is equal to the heat capacity of the humid air. This constant numerical value is about 0.26 to 0.27 for a wet bulb thermometer with water. The purpose of this paper is to show that this value changes with some properties and investigate the correct value for a liquid desiccant. Hence, the Lewis correlation will be summarized, and the agreements and disagreements will be discussed. Then the Lewis correlation will be modified to include the effect of the change in the interfacial temperature with the height of the tower.

2 Materials and Methods

2.1 Correction of Lewis Relation

The basic theory of cooling tower operation was proposed in 1923 by Walker, Lewis, and McAdams [1]. Lewis [2], by assuming the interface temperature to be constant with respect to tower height, was able to develop an approximate relation to describe cooling water systems. Merkel [3] combined Lewis' relation with the equations for heat and water vapor transfer to show that total heat or enthalpy could be used as a driving force to potentially provide both sensible and latent heat transfer. Merkel's work explained the insignificance of inlet air dry–bulb temperature in determining the cooling obtained in a given tower with specified air and water rates. Merkel's relationship,

$$\frac{h_g}{k_G} = c_s = 0.2355 \pm 0.0006,$$

states that the heat transfer coefficient divided by the coefficient of vapor diffusion through the gas film is constant and equal to the heat capacity of the humid air. This ratio can be calculated from the wet–bulb and dry–bulb temperatures for any vapor—gas mixture of known gas humidity. Clearly h_G and k_G depend on the air film thickness.

In 1933, Lewis [4] noted that the equations derived in 1922 were correct, but in comparing them it was mistakenly assumed that the absolute humidity of water and the temperature of the water was constant, whereas, in fact, they are functions of the air absolute humidity and temperature (Lewis [15]). The assumption by Lewis that the interface temperature is always equal to the liquid temperature is incorrect because the interfacial temperature depends on the air temperature. After many difficulties, he solved the problem through experimentation. He concluded that the ratio of the heat transfer coefficient of the gas to the vapor coefficient of diffusion is 0.60, a value more than 2.5 times greater than the heat capacity of the humid air. Simpson and Sherwood [16] agreed with this value of the psychrometric ratio and with Lewis' assumptions regarding work for a compact cooling tower used for air conditioning. They assumed that the ratio h_G/k_G for the water surfaces in a cooling tower was the same as for a wet–bulb thermometer. However, for a packed tower the mass and heat transfer areas are not equal thus Simpson and Sherwood assumed the psychrometric ratio to be $h_G a_H / k_G a_M$, where a_H is the area of heat transfer and a_M is the interfacial mass transfer area.

Hensel and Treybal [5] also found that the interface temperature and the humidity vary considerably which required that the experimental coefficients had to be corrected before being used to generate a correlation. Further, they noted that the psychrometric ratio for a packed column is neither constant nor equal to the heat capacity of the humid air. They found the same values as Hensel and Treybal [5] reported in air–water systems. This ratio also varies in a packed column in which lithium chloride solutions are concentrated. They concluded that until additional data becomes available, it is recommended that the design of packed columns for this application is based on heat/mass transfer coefficient ratio of about 0.5 Btu/lb°F rather than 0.24 Btu/lb°F.

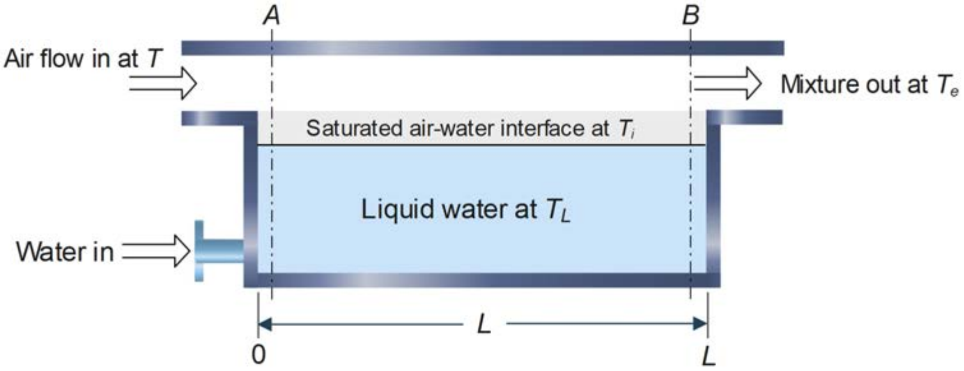

Figure 1: *Configuration considered for analysis (not scaled).*

2.2 New Psychrometric Ratio Value

Consider a long insulated horizontal pipe, as shown in Figure 1 (a detailed experimental setup of this figure will be introduced later), where liquid and air are in contact. The liquid, which is added as needed to maintain a constant level in the container, is stirred constantly to ensure that its concentration and temperature remain the same throughout the container. An air stream is introduced at one end of the container (pipe) over-flows over the liquid and allows the inlet temperature of the liquid to be less than the inlet air temperature. If the channel is long enough, the air stream will exist as saturated air at the adiabatic saturation temperature. The process can be analyzed as a steady–flow process with the mass velocity of the air over the liquid constant and sufficiently low so that heat generated by friction may be neglected. This process involves no heat or work interactions; therefore, the kinetic and potential energy changes may be neglected.

Lewis [2] derived this correlation with a thin layer for a humidifier cooler (1922). Because the process is adiabatic and the only substance getting in and out is air, the following equations can be written for the mass and energy balances at the air and saturated gas layer interface at point A (see Figure 1). The weight of the evaporated liquid is

$$-dW = k_G^{'} a_M (P_i - P) dt \tag{1}$$

where $k_G^{'}$ is the mass of liquid vapor transferred across the interface area, P is the partial pressure of the air, P_i is the partial pressure of the liquid-vapor in the interface, t is time, and a_M is the mass transfer interface area. The sensible and latent heats can be expressed as

$$dQ = h_G a_H (T - T_i) dt \tag{2}$$

and

$$dQ = -\lambda_o dW \tag{3}$$

In Equation (2), h_G is the heat transfer coefficient and a_H is the heat transfer interface area and λ_o in Equation (3) is the latent heat of vaporization at the base temperature of 90°F.
The absolute humidity is given by

$$w = 0.622\phi \frac{P_s}{P_t} \tag{4}$$

where ϕ is the relative humidity ($\phi = P_v/P_s$), P_v is the partial liquid vapor pressure and P_s is the saturated steam vapor pressure at the air temperature. Rearrangement Equation (4) yields,

$$w = 0.622\frac{P_v}{P_t}, \quad \text{and} \tag{5a}$$

$$P = P_v = \frac{1}{0.622}P_t w \tag{5b}$$

Combining and rearranging Equations (1), (2), and (3) yields,

$$(P_i - P) = \frac{h_G a_H}{\lambda_o k_G^{'} a_M}(T - T_i) \tag{6}$$

If the interface is fully wetted, the heat transfer and mass transfer interface areas will be equal to each other ($a_M \approx a_H$). As the liquid temperature is constant throughout the pipe, the condition is fully wetted. Substituting Equation (5b) into Equation (6), rearranging and applying, $a_M \approx a_H$ gives

$$\frac{1}{0.622}k_G^{'}P_t(w_i - w) = \frac{h_G}{\lambda_o}(T - T_i) \tag{7}$$

The product of the first three terms on the left–hand side of Equation (7) is the mass transfer coefficient

$$k_G = \frac{1}{0.622}k_G^{'}P_t \tag{8}$$

Substituting Equation (8) into Equation (7) yields,

$$(w_i - w) = \frac{h_G}{k_G\lambda_o}(T - T_i) \tag{9a}$$

$$\lambda_o dw = -\frac{h_G}{k_G}(T_i - T) \tag{9b}$$

The heat given up by cooling the air must correspond to the heat of the vaporization of water. Hence, it becomes

$$-c_s dT = \lambda_o dw \tag{10}$$

where c_s is the humid air heat capacity, $c_s = 0.24 + 0.45w$ (Btu/lb dry air °F). By assuming c_s and λ_o are constant throughout the pipe and then integrating Equation (10) from point A to point B (see Figure 1), it can be shown that,

$$(w_e - w) = \frac{c_s}{\lambda_o}(T - T_e) \tag{11}$$

where the subscript e indicates the exit. Rewriting Equations (9) and (11) generates the main equation of the Lewis correlation

$$w = w_i - \frac{h_G}{k_G\lambda_o}(T - T_i) = w_e - \frac{c_s}{\lambda_o}(T - T_e) \tag{12}$$

Lewis assumed that the interface temperature did not vary across the tube length. In other words, the interface temperature was equal to the liquid temperature, T_L, everywhere, and he also assumed that at the exit there was a thermal and vapor pressure equilibrium, namely

$$T_i = T_L = T_e, \quad \text{and}$$

$$w_i = w_e$$

By using Equation (12), and the above definitions, we obtain

$$\frac{h_g}{k_G} = c_s \tag{13}$$

The psychrometric ratio, Equation (13), is the same as Lewis' correlation obtained in 1922.

2.3 Modified Lewis Correlation

As previously mentioned, the interface temperature may not necessarily be equal to the liquid temperature. Hensel and Treybal [5], and Lof et al. [6] concluded that the psychrometric ratio varies between 0.23 and 0.58. Hensel and Treybal [5] found the psychrometric ratio equal to 0.58 by assuming an extrapolated tower height. Their results imply that there should be a constant in front of the heat capacity of humid air, c_s. By introducing a correlation constant A to the right side of Equation (15), the modified Lewis correlation can be rewritten in the form of,

$$\frac{h_g}{k_G} = Ac_s \tag{14}$$

In light of the conclusions presented by Hensel and Treybal [5], and Lof et al. [6], A fluctuates between 1 and 2.32. When the layer of the liquid is very thin, it can be assumed that the interface temperature is equal to the liquid temperature. Compared to packed tower applications, the water layer is not thin. Considering the assumption of that the interface temperature depends on the air and liquid temperatures, the following assumption can be made:

$$T_i = A_1 T + A_2 T_L \quad \text{and} \quad \mathrm{A}_1 + \mathrm{A}_2 = 1 \tag{15}$$

For instance, choosing $A_1 = 0$, Equation (15) concludes to $T_i = T_L$. The correlation for the interface temperature may be obtained through experimentation. As mentioned previously, the Lewis correlation was found for a thin water layer, so for a thick water layer Equation (12) must be modified. The liquid film resistance to heat and mass transfer in the air–liquid system can be assumed negligible. The following equation relating to the height of a packed column and the film coefficient in the gas phase was obtained by Lof et al. [6].

$$h_G a_H = \frac{G^{'} c_s}{Z} \ln\left(\frac{T - T_i}{T_e - T_i}\right)$$

Taking into account of the long horizontal pipe, the above equation can be written as:

$$h_G a_H = \frac{G^{'} c_s}{L} \ln\left(\frac{T - T_i}{T_e - T_i}\right) \tag{16}$$

where $G^{'}$ is the flow rate of air, and L is the length of the tube. However, in regard to the tower, the basic differential equation for heat transfer is [6]

$$G^{'} c_s dT = -h_G a_H (T_G - T_i) dz \tag{17}$$

The heat transfer coefficient of the liquid phase is very small compared with the heat transfer coefficient of the gas phase, hence assuming

$$h_{overall} \approx h_G \quad \text{and} \quad (a_H)_{overall} \approx (a_H)_G \tag{18}$$

Now considering the overall heat transfer, Equation (17) can be modified to

$$-h_{overall}(a_H)_{overall}(T_G - T_L)dz = G^{'} di_G \tag{19}$$

where air enthalpy difference is given by

$$di_G = c_s dT_G + \lambda_o dw_G$$

The temperature difference between air and liquid will change throughout the tower, namely;

$$\Delta T \neq \Delta T(z)$$

The temperature difference throughout the pipe is

$$(\Delta T)_{DF} = \left(\frac{T_e + T_p}{2}\right) - \left[\frac{(T_L)_e + (T_L)_p}{2}\right]$$

where the subscript p indicates a particular point at the pipe and the subscript e represents the pipe exit. Integrating Equation (19) throughout the pipe (see Figure 1),

$$\int_0^L -h_{overall}(a_H)_{overall}(T_G - T_L)dz = \int_p^e G^{'} di_G \tag{20}$$

yields,

$$-h_{overall}(a_H)_{overall}(\Delta T)_{DF} L = G^{'} \left\{[c_s(T_e - T_o) + \lambda_o w_e)] - [c_s(T - T_o) + \lambda_o w]\right\} \tag{21}$$

where T_o is the base temperature (90°F). Rearranging Equation (21)

$$-h_{overall}(a_H)_{overall}(\Delta T)_{DF} L = G^{'} \left[c_s(T_e - T) + \lambda_o(w_e - w)\right] \tag{22}$$

From Equation (22), the absolute humidity difference can be written as

$$w_e - w = \frac{c_s}{\lambda_o}(T - T_e) + \frac{1}{G^{'}\lambda_o}\left[-h_{overall}(a_H)_{overall} L(\Delta T)_{DF}\right] \tag{23}$$

Substituting Equations (16) and (18) into Equation (23), we obtain

$$w_e - w = \frac{c_s}{\lambda_o}(T_e - T) + \frac{c_s}{\lambda_o}(\Delta T)_{DF} \ln\left(\frac{T - T_i}{T_e - T_i}\right) \tag{24}$$

Equation (9) is just for the conditions where the gas temperature is greater than the liquid temperature. Taking the absolute value of the temperature difference of Equation (9) makes it valid for $T_L > T_G$. Relating this and Equation (24), the modified main equation of the Lewis correlation becomes:

$$w = w_i - \frac{h_g}{k_G \lambda_o}\left|T - T_i\right| = w_e + \frac{c_s}{\lambda_o}(T_e - T) - \frac{c_s}{\lambda_o}(\Delta T)_{DF} \ln\left(\frac{T - T_i}{T_e - T_i}\right) \tag{25}$$

Equation (25) is valid for the long horizontal pipe. Substituting Equations (5a) and 5(b) into Equation (25), the modified psychrometric ratio of the packed tower for water can be obtained as

$$\begin{aligned}\frac{0.622}{P_t} c_2 (T_i)_p \quad &- \quad \frac{h_G}{k_G \lambda_o}\left|T_p - (T_i)_p\right| = \frac{0.622}{P_t} c_2 T_e + \frac{c_s}{\lambda_o}(T_e - T_p) \\ &+ \quad \frac{c_s}{\lambda_o}\left\{\left[\frac{(T_L)_e + (T_L)_p}{2}\right] - \left(\frac{T_e + T_p}{2}\right)\right\} \ln\left|\frac{T_p - (T_i)_p}{T_e - (T_i)_e}\right|\end{aligned} \tag{26}$$

Rearranging Equation (26) yields

$$\frac{h_G}{k_G} = \frac{\frac{0.622}{p_t} c_2\left[(T_i)_p - T_e\right] + \frac{c_s}{\lambda_o}(T_p - T_e) - (\Delta T)_{DF} \ln\left|\frac{T_P - (T_i)_p}{T_e - (T_i)_e}\right|}{\left|T_p - (T_i)_p\right|} \lambda_o \tag{27}$$

where $c_2 = 4.622\text{E–}2$ and $\lambda_o = 1042$ for the saturated pressure between 90°F and 145°F and $P_t = 13.05$ psi. Constant A, for this case, can be found by dividing Equation (27) by c_s.

2.4 Determination of Coefficient A for a Liquid Desiccant

Desiccants are used to absorb moisture from the air, thus keeping the humidity level in the air to A required value. Since first developed by Lof in 1955, the desiccant dehumidification system has been extensively used in industrial and agricultural sectors [17]. Many researchers investigated to improve the effectiveness of liquid desiccants [18]. Ertas et al. [19] develop a new desiccant called CELD (Cost Effective Liquid Desiccant)– is a mixture of calcium chloride and lithium chloride. The mixture solution was tested between 26.6 °C to 65.6 °C with a concentration from 20wt% to 40wt%. The testing results indicated that mixing LiCl with $CaCl_2$ reduces the vapor pressure in a nonlinear manner in the tested temperature range. They also showed that a mixture of 50% calcium chloride and 50% lithium chloride (CELD) will reduce the cost of the adsorption process. The effectiveness of liquid and solid desiccant dehumidification systems was investigated for air conditioning and agricultural product drying and compared by Naik et al. [20]. They found that the highest latent effectiveness and dehumidification ability were at the desorption temperature of 345 K, at 0.91 and 6.8 g/kg, respectively. The use of liquid desiccant for industrial applications was investigated by Ertas et al. [21, 22].

The effect of the latent heat on the performance of the desiccant dehumidification system for five different desorption temperatures of 308, 318, 328, 338, and 345 K was experimentally investigated by Yaningsih et al. [23]. Ahn and Choi [24] studied local measurement and computational fluid dynamics (CFD) employed to evaluate thermal comfort in a residential environment where desiccant cooling is performed in Korea.

Analytical and experimental investigations on liquid desiccant systems for drying air or air conditioning systems were studied by Xiaochen et al. [25], Hesam [26], and Esam [27] among the many other researchers.

Now consider the liquid pool shown in Figure 2 to be a liquid desiccant. For the case of a long insulated channel above the liquid, the coefficient A for a desiccant is greater than for water. This increase in A results from the increase in resistance to mass transfer which provide a decrease in the mass transfer coefficient. As the mass transfer coefficient decreases, the value of A increases. The value of A for water is in the range of 1 to 2.32; for the desiccant, A is greater than 2.32. The desiccant must be at a higher temperature than the air for regeneration to occur. If the temperature of the air throughout the long channel where the wet–bulb and dry–bulb temperatures are the same, the exit air temperature can be found. If wet–bulb and dry–bulb temperatures are equal, the air is saturated. The exit temperature of air can be assumed to be

$$T_e = c_1^{''} + c_2^{''} T_L \tag{28}$$

where $c_1^{''}$ and $c_2^{''}$ are coefficients that depend on the desiccant concentration. The saturation pressure at the exit can be expressed in terms of the exit temperature as

$$P_{Se} = c_1 + c_2(c_1^{''} + c_2^{''} T_L)$$

Rearranging the above equation provides the saturation pressure at the exit.

$$P_{Se} = c_1 + c_2 c_1^{''} + c_2 c_2^{''} T_L \tag{29}$$

Substituting Equation (29) into the relative humidity equation, Equation (5a), the absolute humidity at the exit can be expressed as

$$w_e = \frac{0.622}{P_t}(c_1 + c_2 c_1^{''} + c_2 c_2^{''} T_L) \tag{30}$$

Substituting Equations (28), (29), and (30) into Equation (27) produces the following psychrometric ratio for regeneration in packed towers.

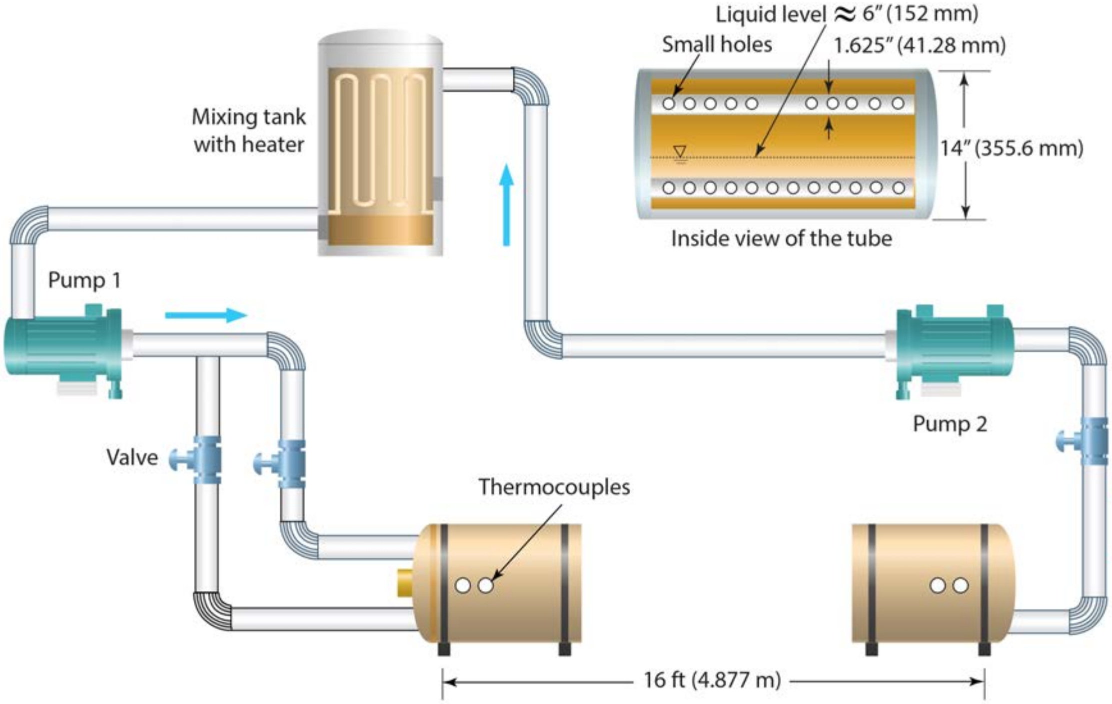

Figure 2: *Experimental set-up (not scaled).*

$$
\begin{aligned}
\frac{h_G}{k_G} &= \frac{\lambda_o}{|T_p-(T_i)_p|}\left\{\frac{0.622}{P_t}c_2\left[(T_i)_p-c_2c_1^{''}+c_2c_2^{''}T_L\right]+\frac{c_s}{\lambda_o}(T_p-c_1^{''}+c_2^{''}T_L)\right\} \\
&+ \frac{\lambda_o}{|T_p-(T_i)_p|}\left\{\left[\frac{(T_L)_e+(T_L)_p}{2}-\frac{c_1^{''}+c_2^{''}T_L+T_P}{2}\right]\ln\left|\frac{T_p-(T_i)_p}{c_1^{''}+c_2^{''}T_L-(T_i)_e}\right|\right\}
\end{aligned}
\tag{31}
$$

Constant A can be found by dividing Equation (31) by c_s. Equation (31) is the general form for the psychrometric ratio. It is obvious that the water has no concentration. Substituting $c_1^{''}$=0 and $c_2^{''}=1$ reduces Equation (31) to the case for liquid water for packed towers or Equation (27).

2.5 Experimental Set-Up

To find the psychometric ratio for the water and desiccant, two experiments were performed. The tube was long enough to allow the mixture to reach the same wet and dry temperature. After measuring the temperatures for particular desiccant concentrations, a correlation for the exit air temperature as a function of the desiccant temperature was found for the range of the concentrations considered.

A 4877 mm long pipe (tube) with 355.6 mm diameter, shown in Figure 2, contained a desiccant at high temperature and air at ambient temperature. The following test procedures were used to perform the experiment.

- The flow rate of the liquid was carefully adjusted.
- Two small diameter (41.28 mm), 4877 mm long pipes of an equal length as the large pipe was constructed with many small holes along their sides. These holes were used to mix the desiccant constantly so that its concentration and temperature were nearly constant throughout the large pipe.

- The heater in the mixing tank was used to bring the desiccant to a particular temperature and then turned off while the flow continued. When the thermocouples located at ports along the tube indicated the same value, the experiment for that temperature was started.
- The pumps, which were used to pump the desiccant to and from the tube had similar characteristics to control the flow.
- Valves were used to adjust the level of the desiccant in the tube and to keep the flow rate constant.
- Regular tap water is used and the level of the water assumed to be flat.
- Thermocouples were installed at a distance of very little over the water level of 152 mm.

The flow rate of the air, as well as the flow rate of the desiccant, during the experiment, is important. If a very high airflow rate is used, the wet and dry bulb temperatures can never be equal. Therefore, a constant low air flow rate was used. Although the air flow rate, the length of the tube, etc., are not related to the psychometric ratio, they were adjusted to find equal wet and dry bulb temperatures in the tube. Because the flow rate of air is not a parameter for the psychometric ratio, it was not measured.

One of the other major problems was to keep the concentration constant because it became higher as the temperature increased. Before making each experiment at a specific temperature, the heaters were turned off, and the concentration of the desiccant was measured and brought to the desired level.

A hydrometer, which gives reliable accuracy to the third decimal place, was used to determine the density of the CELD. The test procedure for the CELD density measurement is as follows:

1. Carefully clean and dry the hydrometer.
2. Make sure the temperature of the hydrometer is at the same temperature as the solution temperature.
3. Mix the solution well enough to ensure uniformity and pour into a graduated cylinder.
4. Place the graduated cylinder into a constant temperature bath.
5. Dip the hydrometer slowly in the solution and then release it to float freely.
6. Record reading.

After finding the value of the density, d, the concentration equations for specific temperatures were used to find the concentration of the desiccant. Some of them are:

$$\begin{aligned}
&\text{at}\quad 90^\circ F \qquad C = -134.473 + 138.261d;\\
&\text{at}\quad 100^\circ F \qquad C = -134.197 + 138.261d;\\
&\text{at}\quad 110^\circ F \qquad C = -133.920 + 138.261d;\\
&\text{at}\quad 160^\circ F \qquad C = -132.539 + 138.261d;
\end{aligned}$$

In all these equations, the density is in SI units.

The experiment was started with a high CELD concentration of 46% and lowered to 38.2% during the experiment. In other words, the experiments were run for five concentrations (38.2%, 40%, 42%, 44%, 46%) at specific temperatures. To measure temperatures accurately, the thermocouples were calibrated. The procedure of the calibration is as follows.

- The thermocouples and an accurate thermometer were submersed in a large cup filled with water. The temperatures for each were recorded.
- The cup was heated slowly while the thermocouple and thermometer readings were recorded. The water temperature varied over the range of temperatures anticipated during the experiments.

Table 1. Experimental results depending on concentration.

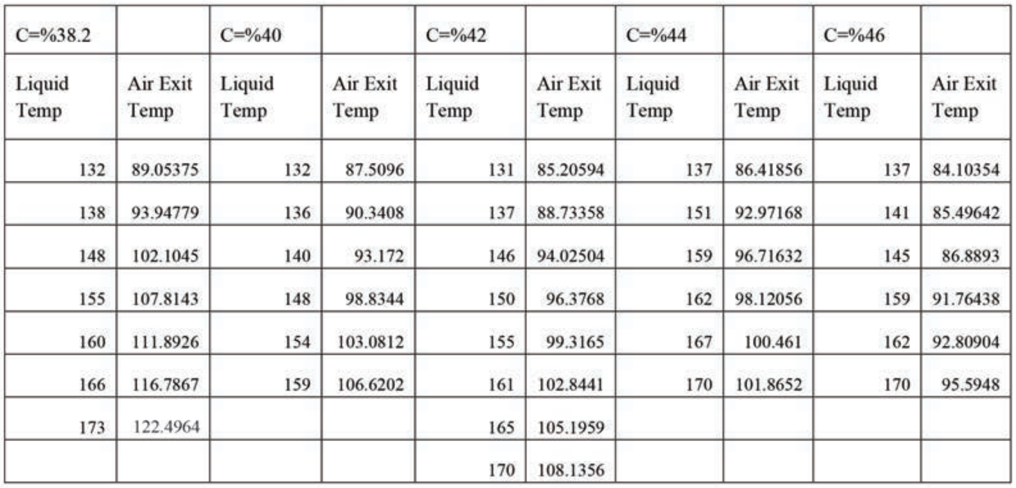

C=%38.2		C=%40		C=%42		C=%44		C=%46	
Liquid Temp	Air Exit Temp	Liquid Temp	Air Exit Temp	Liquid Temp	Air Exit Temp	Liquid Temp	Air Exit Temp	Liquid Temp	Air Exit Temp
132	89.05375	132	87.5096	131	85.20594	137	86.41856	137	84.10354
138	93.94779	136	90.3408	137	88.73358	151	92.97168	141	85.49642
148	102.1045	140	93.172	146	94.02504	159	96.71632	145	86.8893
155	107.8143	148	98.8344	150	96.3768	162	98.12056	159	91.76438
160	111.8926	154	103.0812	155	99.3165	167	100.461	162	92.80904
166	116.7867	159	106.6202	161	102.8441	170	101.8652	170	95.5948
173	122.4964			165	105.1959				
				170	108.1356				

- The data for each thermocouple was curve-fit and a graph was produced for the temperature of each thermocouple versus the temperature of the thermometer.
- For convenience during testing, a table for each thermocouple between the temperatures of 80 °F and 180 °F was prepared.

Along the tube, two holes (just above the liquid level of 152 mm) were drilled every 2 feet for the thermocouples. The thermocouples for dry bulb temperatures at each port were placed ahead of the thermocouples for wet bulb temperatures. One end of a section of shoestring was placed over each wet bulb temperature thermocouple and the other end was placed in a small container that contained water. Throughout the experiment, care was taken to ensure that the container was filled with water so that the hole and the string were always wet.

After considering all of the experimental parameters, the system was built and initially tested with water rather than desiccant to check for leaks, constant liquid temperature, and flow rate throughout the tube.

3 Results and Discussions

At the completion of each test, the data for each desiccant concentration was reviewed and plotted. Data for the tests that produced the same wet and dry bulb temperatures for each desiccant concentration are tabulated in Table 1. Figure 3 shows the experimental results generated using Table 1.

For desiccant concentrations at low temperatures, equilibrium was expected near the ports at the exit of the tube, and as the temperatures of the liquid increased equilibrium was expected to move toward at front ports on the tube. However, for many tests equilibrium occurred at a port about 14 feet from the entrance. At low concentrations, a steady state was obtained in a short time. Increasing the percent of the concentration, especially at high temperatures, presented a great deal of difficulty in obtaining steady state conditions due to the time required. Therefore, tests for 46% desiccant concentration were repeated three times, and two of the results were dropped by considering the slope of the other concentrations.

From the experimental data, a correlation was obtained using the SAS software for the Equation (3.28), where $c_1^{''}$ and $c_2^{''}$ depend on the concentration, C. The correlation for Equation (28) is:

$$T_e = (-288.036 + 705.29C) + (3.105 - 5.993C)T_L \tag{32}$$

Figure 4 was generated from Equation (32).

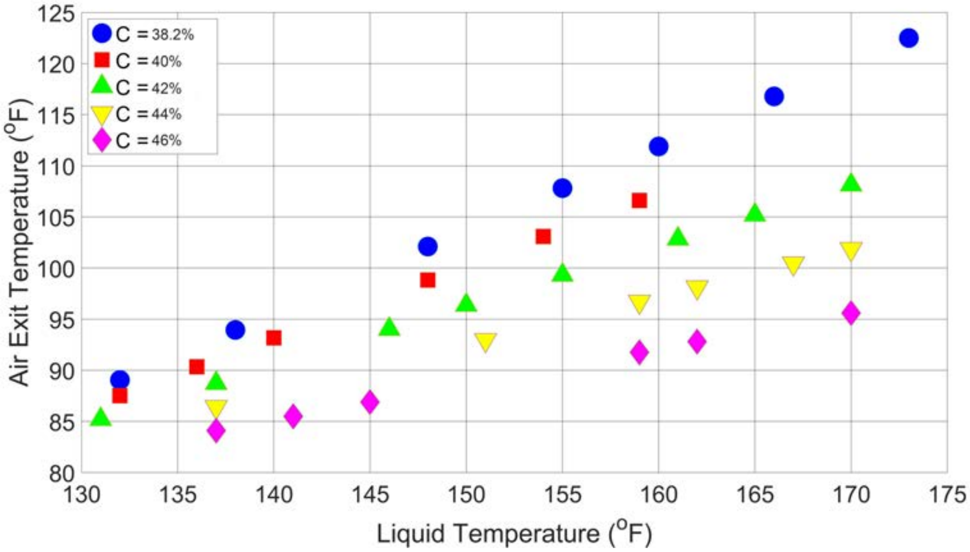

Figure 3: *Experimental results generated using Table 1.*

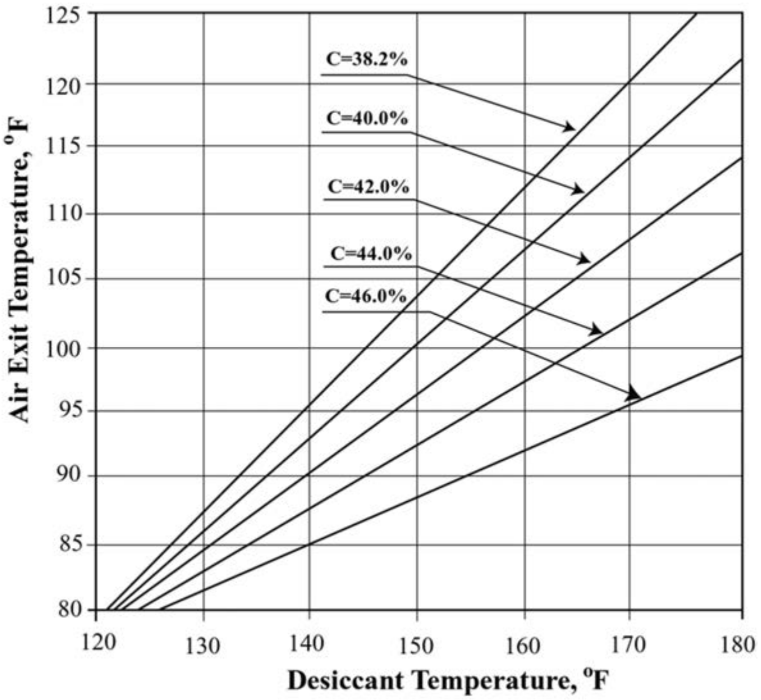

Figure 4: *Experimental results for exit air temperature by using correlation.*

Table 2: *Experimental results for interface temperature.*

Water temperature (°F)	Air temperature (°F)	Interface temperature (°F)
102.5	81.8	100.7
103.5	82.3	102.0
105.6	82.3	104.2
107.0	83.5	105.4
109.1	84.3	107.3
110.4	84.5	108.5
112.2	84.8	110.5
114.5	85.4	112.7
116.3	85.9	114.2
118.8	86.2	116.6
120.2	86.6	117.9
121.9	86.9	119.6
123.4	87.3	121.1

The second experiment was conducted, using the same experimental set-up, to find a correlation for the interface temperature of the water. The air and interface temperatures were measured for a given air flow rate and different water temperatures. Thermocouples used to measure the interface temperature were fixed on a small and thin metal tab. The approximate interface temperatures were measured by placing half of the metal tab in the water and half in the air. The results of this experiment are presented in Table 2. The correlation obtained for the interface water temperature is

$$T_i = 0.94T_L + 0.058T_G \tag{33}$$

Figure 5 was generated using experimental results shown in Table 2. The measured interface temperatures were approximately two degrees lower than the water temperatures. The same correlation can be used for desiccant applications because the transfer media between the air and the desiccant is water.

Case 1: By taking account of thermal and vapor pressure equilibrium at the exit, ($T_i = T_L = T_e$), and $w_i = w_e$ and rearranging Equation (28), the psychrometric ratio can be obtained for the case of water with thermal and vapor pressure equilibrium. The value of the constant A can then be found by dividing c_s by the psychrometric ratio. Table 3 (see Appendix A) presents the MATLAB example algorithm used to compute the value of A for this case. Using Kiris' [23] experimental data (see Appendix A, Table 7) in this algorithm for a humidifier, the constant A found to be 1.226 (see Table 3).

Typically, a tower is not tall enough to produce thermal and vapor pressure equilibrium at the exit. However, results can be found from the psychrometric ratio, determined from the interface temperature correlation. A MATLAB example algorithm to compute A=1.799 for this case is shown in Table 4 (see Appendix A) .

Case 2: Substituting Equations (32) and (33) into Equation (31) and using the data for regeneration (Table 6) by Kiris [29], the psychrometric ratio can be found. Dividing the value of this ratio to the heat capacity of humid air which is equal to 0.25, the constant A=13.573 can be obtained ((see Appendix A Table 5 for the MATLAB algorithm to compute constant A for CELD).

4 Conclusion

In this study, air and liquid contact for humidifier and regeneration applications have been carried out. Considering the psychrometric ratio change between 0.25 and 0.58, the modified Lewis correlation for water

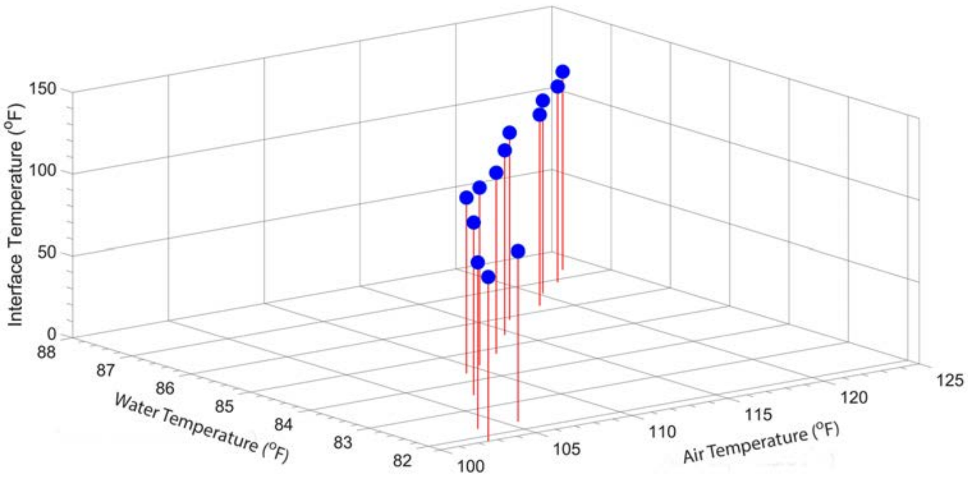

Figure 5: *Experimental results of interface temperatures.*

and liquid desiccant (CELD) was derived. To find the psychometric ratio for the water and desiccant, two experiments were performed. After measuring the temperatures for particular desiccant concentrations, a correlation for the exit air temperature as a function of the desiccant temperature was found for the range of the concentrations considered. The following conclusions were drawn from this study:

1. In the Lewis relation for a very thin water layer the psychrometric ratio is equal to the heat capacity of the humid air. If the layer is not thin, the psychrometric ratio will be changed in the range of 0.25 and 0.58.
2. A correlation for the interface temperature for water was found. This correlation can also be used for desiccant because the transfer media between air and desiccant is water.
3. An experiment for the desiccant was performed. A correlation for the exit air temperature depending on the concentration and liquid temperature was obtained. Using the interface temperature and air exit temperature correlations, the modified psychrometric ratio A for the following cases was obtained:

   - A= 1.226 for the case of water with thermal and vapor pressure equilibrium,
   - A= 1.799 based on the experimental interface temperature correlation, and
   - A= 13.573 for regeneration of CELD.

The followings are recommendations for future work in this research area: (a) obtain the results for different air and desiccant flow rates, (b) perform experiments by changing the air flow rate for humidifier and regeneration to obtain correlations.

Acknowledgments

We would like to take this opportunity to thank Dr. Ilker Kiris for his insightful comments.

Abbreviations

The following abbreviations are used in this manuscript:

a_H	Interfacial heat transfer area, ft^2/ft^3
a_M	Interfacial mass transfer area, ft^2/ft^3
c_s	Heat capacity of humid air, BTU/(lbm°F)
d	Density of desiccant, lbm/ft^3
ϕ	Relative humidity of air
G'	Dry air mass velocity, lbm dry air/(min ft^2)
h	Film heat transfer coefficient, BTU/(°F ft^2 min)
h_G	Heat transfer coefficient of gas phase, BTU/(°F ft^2 min)
$h_{overall}$	Overall heat transfer coefficient, BTU(°F ft^2 min)
i	Enthalpy of mixture of air and water vapor at given T, BTU/lbm of dry air
k	Film mass of enthalpy transfer coefficient, Btu/(min ft^2 (Btu/lbm))
k_G	Mass transfer coefficient of the liquid phase, Btu/(min ft^2 (BTU/lbm))
λ_o	Latent heat of vaporization of water at base temperature T_0, BTU/lbm
P	Partial liquid vapor pressure of the air, lbf/ft^2
P_i	Partial liquid vapor pressure of the interface, lbf/ft^2
P_v	Partial liquid vapor pressure, lbf/ft^2
P_s	Saturated steam vapor pressure, lbf/ft^2
t	Time, min
T	Air temperature, °F
T_e	Air temperature at exit, °F
T_G	Bulk air temperature, °F
T_i	Interface temperature, °F
T_L	Liquid temperature, °F
T_p	Air temperature at particular height of the tower, °F
$(\Delta T)_{DF}$	Temperature difference throughout the pipe, °F
$(T_i)_e$	Interface temperature at the exit of the tower, °F
$(T_i)_p$	Interface temperature at the particular height of the tower, °F
$(T_L)_e$	Liquid temperature at the exit of the tower, °F
$(T_L)_p$	Liquid temperature at the particular height of the tower, °F
w	Absolute humidity, (lbm H2O)/(lbm dry air)
w_e	Absolute humidity at the exit tower, (lbm H_2O)/(lbm dry air)
W	Weight of evaporated liquid, lbm (H_2O)
Z	Height of packing materials, ft

Subcripts

G	Bulk gas
H	Heat transfer
I	Gas liquid interface
L	Bulk liquid (CELD)
M	Mass transfer
W	Water

Funding: This research received no external funding.

Conflicts of Interest: The authors declares no conflict of interest.

Authors Contributions: This work is Mr. Gurses' MS thesis. Dr. Ertas was Mr. Gurses' advisor.

References

[1] Lewis, W. K. McAdams, W. H. (1937). *Principles of Chemical Engineering*, 3rd Edition, McGraw–Hill, New York.

[2] Lewis, W. K. (1992). *Trans. American Society of Mechanical Engineers*, Vol. 44, pp.379.

[3] Treybal, R. E. (1980). *Mass–Transfer Operation*, 3rd Edition, McGraw–Hill, New York.

[4] Lewis, W. K. (1933). The Evaporation of a Liquid into a Gas–A Correction. *Mechanical Engineering* **1933**, Vol. 55, pp. 565–573.

[5] Hensel, S. L., Jr. and Treybal, R. E. (1952). Adiabatic Humidification of Air with Water in a Packed Tower. *Chemical Engineering Progress*, pp. 362–370.

[6] Lof, G. O. G., Lenz, T. G. and Rao, S. (1984). Coefficients of Heat and Mass Transfer in a Packed Bed Suitable for Solar Regeneration of Aqueous Lithium Chloride Solutions. *Journal for Solar Energy Engineering*, Vol.106, pp. 387–392.

[7] Strigle, R. F., Jr. (1987). *Random Packings and Packed Towers: Design and Application.* Gulf Publishing Company, Houston, Texas.

[8] McAdams, W. H., Phlenz, J. B. And John, R. C. (1949). Transfer of Heat and Mass between Air and Water in a Packed Tower. *Chemical Engineering in Progress*, Vol. 45, No. 4, pp. 241–252.

[9] Sherwood, T. K. and Holloway, F. A. L. (1939). Performance of Packed Towers – Experimental Studies of Absorption and Desorption. *Transactions American Society of Engineers,* p.21.

[10] Molstad, M. C., Abbey, R. G., Thompson, A. R. and McKinney, J. F. (1942). Performance of Drip–Point Grid Tower Packings II. Liquid–Film Mass Transfer Data. *Transactions American Chemical Engineering*, Vol. 38, 410–434.

[11] Vivian, J. E., and Whitney, R. P. (1949). Absorption of Sulfur Dioxide in Water, *Chemical Engineering Progress,* Vol. 45, 323–337.

[12] Norman W. S. (1961). Absorption, Distillation and Cooling Towers, Wiley, New York.

[13] Sherwood, T. K. and Pigford, R. L. (1952). *Absorption and Extraction*, 2nd Edition, McGraw–Hill, New York.

[14] Puranik, S. S. and Vogelpohl, A. (1974). Effective Interfacial Area In Irrigated Packed Columns. *Chemical Engineering Science*, Vol. 29, pp. 501–507.

[15] Lewis, W. K.(1984). The Evaporation of a Liquid into a Gas–A Correction *Mechanical Engineering*, Vol. 55, pp. 153–158.

[16] Simpson, W. M. and Sherwood, T. K. (1946). Performance of Small Mechanical Draft Cooling Towers. *Journal of the ASREA*, pp. 535–576.

[17] GOG, L. (1955). Cooling with solar energy. Congress on Solar Energy, Tucson, Ariz, pp. 73–78.

[18] Xiangjie, C., Saffa, R., Hongyu, B., Xiaofeng, Z., Reay, D. (2020). Recent progress in liquid desiccant dehumidification and air-conditioning: A review. *Energy and Built Environment*, 1, 106–130.

[19] Ertas, A., Anderson, E. E., Kiris, I. (1992). Properties of a new liquid desiccant solution–Lithium chloride and calcium chloride mixture. *Solar Energy,* 49 (3), 205–212.

[20] Naik,B. Kiran, Mullapudi, J., Palanisamy,M., Muhammad, S., Takahiko, M., Redmond, R. S., and Hadeed, A. 2020. Investigating Solid and Liquid Desiccant Dehumidification Options for Room Air-Conditioning and Drying Applications. *Sustainability*, 12, 10582; doi:10.3390/su122410582

[21] Ertas, A., Anderson, E. E., Kavasogullari, S. (1991). Comparison of Mass and Heat Transfer Coefficients of Liquid-Desiccant Mixtures in a Packed Column. *Journal of Energy Resources,* 113(1), https://doi.org/10.1115/1.2905774

[22] Ertas, A., Hoque, A. K. A., I. Kiris, I., & P. Gandhidasan, P. (1997). Low Temperature Peanut Drying Using Liquid Desiccant System Climatic Conditions. *Drying Technology*, Vol. 15, Issue 3-4.

[23] Yaningsih, I., Wijayanta, T. A., Thu, K., and Miyazaki, T. (2020). Influence of Phase Change Phenomena on the Performance of a Desiccant Dehumidification System. *Appl. Sci.* 10, 868; doi:10.3390/app10030868

[24] Ahn, J., and Yup Choi H.(2020). Effects of Supply Angle on Thermal Environment of Residential Space with Hybrid Desiccant Cooling System for Multi-Room Control. *Appl. Sci.* 10, 7271; doi:10.3390/app10207271

[25] Liu, X., Liu, X., Zhang, T. (2018). Experimental analysis and performance optimization of a counter-flow enthalpy recovery device using liquid desiccant. *Engineering Sage Journal,* https://doi.org/10.1177/0143624418780852

[26] Salarian, H. (2013). An Analysis of Packed Bed Liquid Desiccant System. *Applied Mechanics and Materials*, 390:680-DOI:10.4028/www.scientific.net/AMM.390.680

[27] Elsarrag E. (2018). An Innovative Smart Liquid Desiccant Air Conditioning System for Indoor and Outdoor Cooling using Seawater Bittern. *Innovative Energy & Research,* Vol 7(1): 178.

[28] Kiris, I. Experimental Development and Investigation of a New Liquid Desiccant System for Drying Operations, M. S. Thesis, Texas Tech University, 1991.

[29] Mickley, H. S. (1949), Design of Forced Draft Air Conditioning Equipment. *Chemical En-gineering in Progress*, Vol.45, No.12, pp. 739–745.

About the Authors

Huseyin M. Gurses is the founding partner of GONCA OSGB, which was established in 2011. He has been the Occupational Health and Safety Director of GONCA OSGB since the day it was founded.

Dr. Atila Ertas is the director of the Academy of Transdisciplinary Studies and a professor of Mechanical Engineering at Texas Tech University. Dr. Ertas has many years of experience in teaching transdisciplinary design courses. He is the author/co-author of over 190 technical papers that cover many engineering technical fields. His textbooks include *The Engineering Design Process* (co-author with J. Jones, 1993, 1996), *Prevention through Design (PtD): Transdisciplinary Process* (2010), *Engineering Mechanics and Design Applications: Transdisciplinary*

Engineering Fundamentals (2011), *Transdisciplinarity Engineering Design Process* (2018), and *Managing System Complexity through Integrated Transdisciplinary Design Tools* (co-author with U. Gulbulak, 2020).

Appendix A

Table 3. MATLAB algorithm to compute the value of constant *A* for the case of water with thermal and vapor pressure equilibrium.

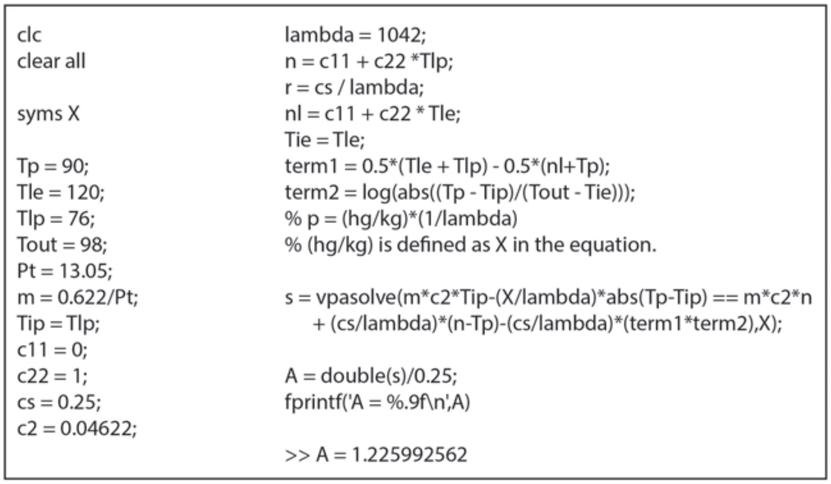

```
clc
clear all

syms X

Tp = 90;
Tle = 120;
Tlp = 76;
Tout = 98;
Pt = 13.05;
m = 0.622/Pt;
Tip = Tlp;
c11 = 0;
c22 = 1;
cs = 0.25;
c2 = 0.04622;

lambda = 1042;
n = c11 + c22 *Tlp;
r = cs / lambda;
nl = c11 + c22 * Tle;
Tie = Tle;
term1 = 0.5*(Tle + Tlp) - 0.5*(nl+Tp);
term2 = log(abs((Tp - Tip)/(Tout - Tie)));
% p = (hg/kg)*(1/lambda)
% (hg/kg) is defined as X in the equation.

s = vpasolve(m*c2*Tip-(X/lambda)*abs(Tp-Tip) == m*c2*n
    + (cs/lambda)*(n-Tp)-(cs/lambda)*(term1*term2),X);

A = double(s)/0.25;
fprintf('A = %.9f\n',A)

>> A = 1.225992562
```

Table 4. MATLAB algorithm to compute the value of constant *A* based on the experimental interface temperature correlation.

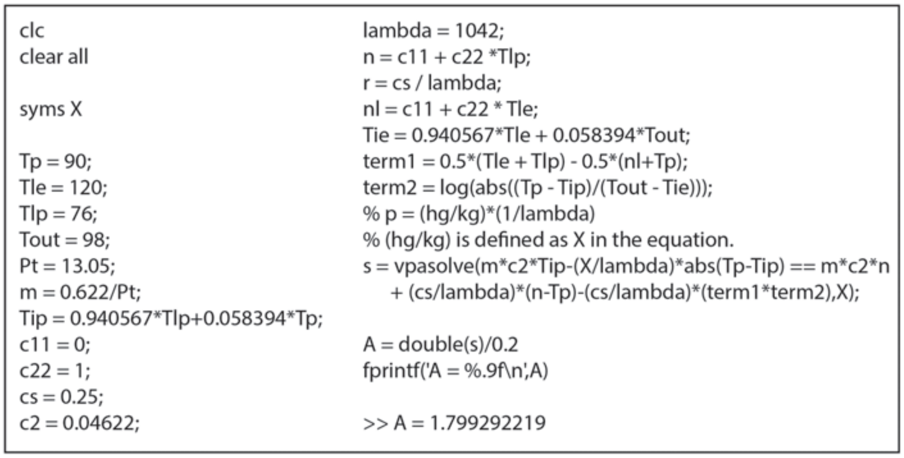

```
clc
clear all

syms X

Tp = 90;
Tle = 120;
Tlp = 76;
Tout = 98;
Pt = 13.05;
m = 0.622/Pt;
Tip = 0.940567*Tlp+0.058394*Tp;
c11 = 0;
c22 = 1;
cs = 0.25;
c2 = 0.04622;

lambda = 1042;
n = c11 + c22 *Tlp;
r = cs / lambda;
nl = c11 + c22 * Tle;
Tie = 0.940567*Tle + 0.058394*Tout;
term1 = 0.5*(Tle + Tlp) - 0.5*(nl+Tp);
term2 = log(abs((Tp - Tip)/(Tout - Tie)));
% p = (hg/kg)*(1/lambda)
% (hg/kg) is defined as X in the equation.
s = vpasolve(m*c2*Tip-(X/lambda)*abs(Tp-Tip) == m*c2*n
    + (cs/lambda)*(n-Tp)-(cs/lambda)*(term1*term2),X);

A = double(s)/0.2
fprintf('A = %.9f\n',A)

>> A = 1.799292219
```

Table 5. MATLAB algorithm to compute the value of constant *A* for regeneration of CELD.

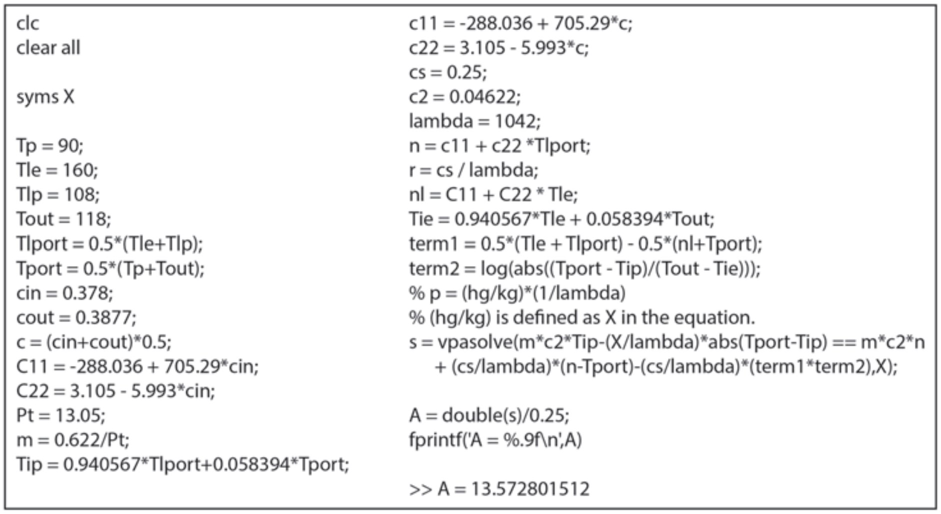

```
clc
clear all

syms X

Tp = 90;
Tle = 160;
Tlp = 108;
Tout = 118;
Tlport = 0.5*(Tle+Tlp);
Tport = 0.5*(Tp+Tout);
cin = 0.378;
cout = 0.3877;
c = (cin+cout)*0.5;
C11 = -288.036 + 705.29*cin;
C22 = 3.105 - 5.993*cin;
Pt = 13.05;
m = 0.622/Pt;
Tip = 0.940567*Tlport+0.058394*Tport;
c11 = -288.036 + 705.29*c;
c22 = 3.105 - 5.993*c;
cs = 0.25;
c2 = 0.04622;
lambda = 1042;
n = c11 + c22 *Tlport;
r = cs / lambda;
nl = C11 + C22 * Tle;
Tie = 0.940567*Tle + 0.058394*Tout;
term1 = 0.5*(Tle + Tlport) - 0.5*(nl+Tport);
term2 = log(abs((Tport - Tip)/(Tout - Tie)));
% p = (hg/kg)*(1/lambda)
% (hg/kg) is defined as X in the equation.
s = vpasolve(m*c2*Tip-(X/lambda)*abs(Tport-Tip) == m*c2*n
    + (cs/lambda)*(n-Tport)-(cs/lambda)*(term1*term2),X);

A = double(s)/0.25;
fprintf('A = %.9f\n',A)

>> A = 13.572801512
```

Table 6. Data sets for regeneration of Kiris with calculated data [23].

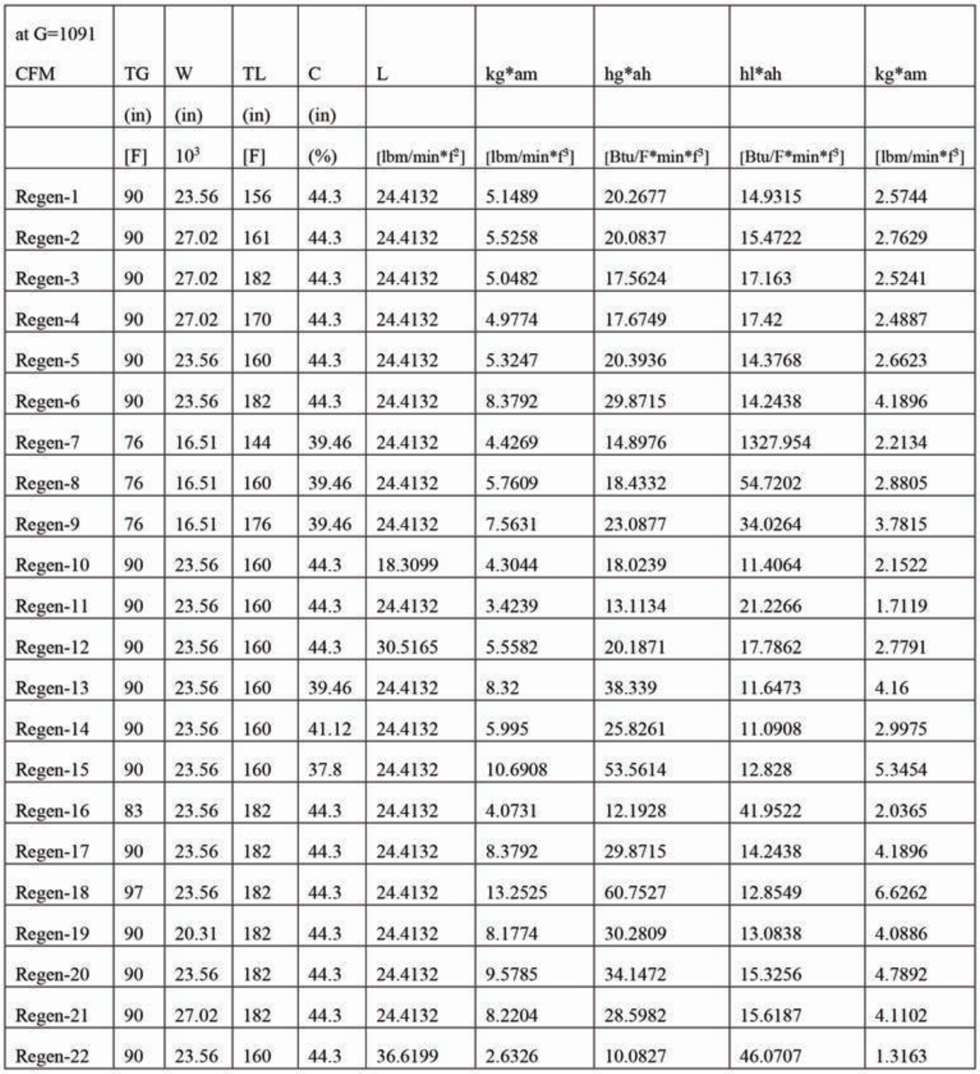

at G=1091 CFM	TG	W	TL	C	L	kg*am	hg*ah	hl*ah	kg*am
	(in)	(in)	(in)	(in)					
	[F]	10^3	[F]	(%)	[lbm/min*f^2]	[lbm/min*f^3]	[Btu/F*min*f^3]	[Btu/F*min*f^3]	[lbm/min*f^3]
Regen-1	90	23.56	156	44.3	24.4132	5.1489	20.2677	14.9315	2.5744
Regen-2	90	27.02	161	44.3	24.4132	5.5258	20.0837	15.4722	2.7629
Regen-3	90	27.02	182	44.3	24.4132	5.0482	17.5624	17.163	2.5241
Regen-4	90	27.02	170	44.3	24.4132	4.9774	17.6749	17.42	2.4887
Regen-5	90	23.56	160	44.3	24.4132	5.3247	20.3936	14.3768	2.6623
Regen-6	90	23.56	182	44.3	24.4132	8.3792	29.8715	14.2438	4.1896
Regen-7	76	16.51	144	39.46	24.4132	4.4269	14.8976	1327.954	2.2134
Regen-8	76	16.51	160	39.46	24.4132	5.7609	18.4332	54.7202	2.8805
Regen-9	76	16.51	176	39.46	24.4132	7.5631	23.0877	34.0264	3.7815
Regen-10	90	23.56	160	44.3	18.3099	4.3044	18.0239	11.4064	2.1522
Regen-11	90	23.56	160	44.3	24.4132	3.4239	13.1134	21.2266	1.7119
Regen-12	90	23.56	160	44.3	30.5165	5.5582	20.1871	17.7862	2.7791
Regen-13	90	23.56	160	39.46	24.4132	8.32	38.339	11.6473	4.16
Regen-14	90	23.56	160	41.12	24.4132	5.995	25.8261	11.0908	2.9975
Regen-15	90	23.56	160	37.8	24.4132	10.6908	53.5614	12.828	5.3454
Regen-16	83	23.56	182	44.3	24.4132	4.0731	12.1928	41.9522	2.0365
Regen-17	90	23.56	182	44.3	24.4132	8.3792	29.8715	14.2438	4.1896
Regen-18	97	23.56	182	44.3	24.4132	13.2525	60.7527	12.8549	6.6262
Regen-19	90	20.31	182	44.3	24.4132	8.1774	30.2809	13.0838	4.0886
Regen-20	90	23.56	182	44.3	24.4132	9.5785	34.1472	15.3256	4.7892
Regen-21	90	27.02	182	44.3	24.4132	8.2204	28.5982	15.6187	4.1102
Regen-22	90	23.56	160	44.3	36.6199	2.6326	10.0827	46.0707	1.3163

Table 7. Data sets for humidifier of Kiris with calculated data [23].

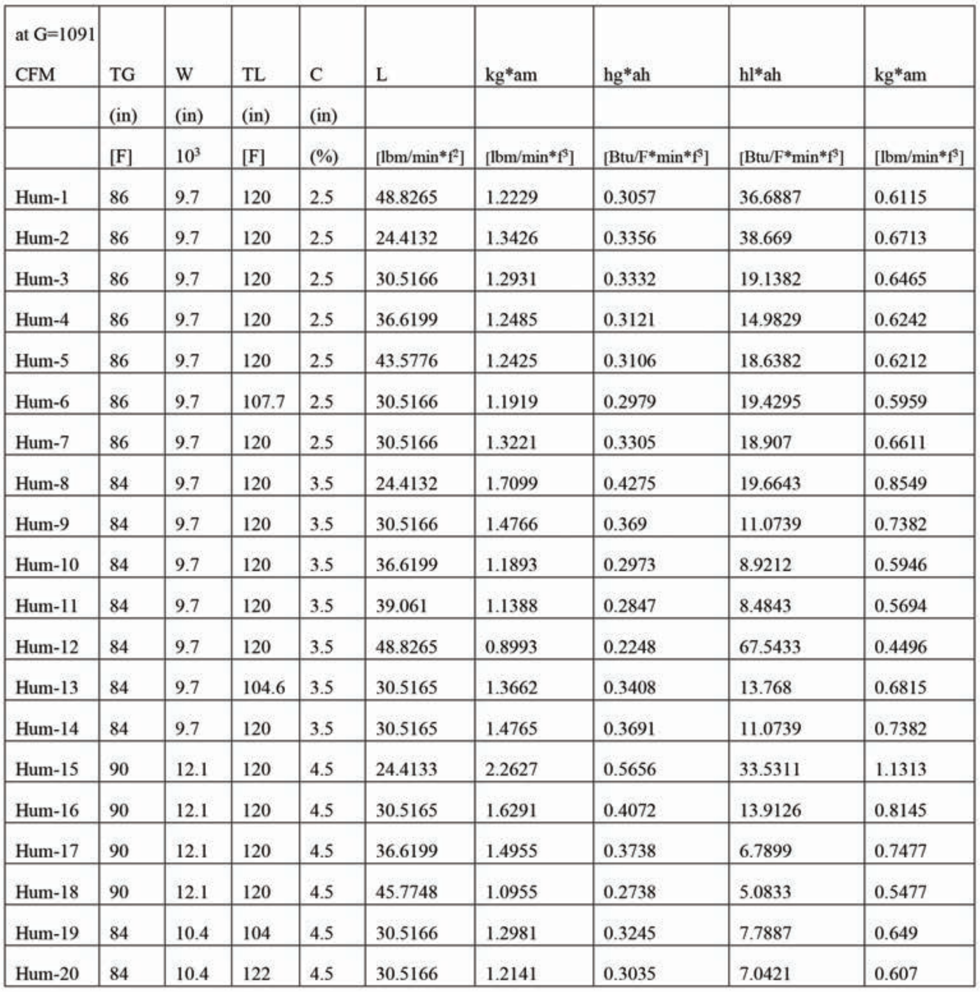

at G=1091 CFM	TG	W	TL	C	L	kg*am	hg*ah	hl*ah	kg*am
	(in)	(in)	(in)	(in)					
	[F]	10^3	[F]	(%)	[lbm/min*f^2]	[lbm/min*f^3]	[Btu/F*min*f^3]	[Btu/F*min*f^3]	[lbm/min*f^3]
Hum-1	86	9.7	120	2.5	48.8265	1.2229	0.3057	36.6887	0.6115
Hum-2	86	9.7	120	2.5	24.4132	1.3426	0.3356	38.669	0.6713
Hum-3	86	9.7	120	2.5	30.5166	1.2931	0.3332	19.1382	0.6465
Hum-4	86	9.7	120	2.5	36.6199	1.2485	0.3121	14.9829	0.6242
Hum-5	86	9.7	120	2.5	43.5776	1.2425	0.3106	18.6382	0.6212
Hum-6	86	9.7	107.7	2.5	30.5166	1.1919	0.2979	19.4295	0.5959
Hum-7	86	9.7	120	2.5	30.5166	1.3221	0.3305	18.907	0.6611
Hum-8	84	9.7	120	3.5	24.4132	1.7099	0.4275	19.6643	0.8549
Hum-9	84	9.7	120	3.5	30.5166	1.4766	0.369	11.0739	0.7382
Hum-10	84	9.7	120	3.5	36.6199	1.1893	0.2973	8.9212	0.5946
Hum-11	84	9.7	120	3.5	39.061	1.1388	0.2847	8.4843	0.5694
Hum-12	84	9.7	120	3.5	48.8265	0.8993	0.2248	67.5433	0.4496
Hum-13	84	9.7	104.6	3.5	30.5165	1.3662	0.3408	13.768	0.6815
Hum-14	84	9.7	120	3.5	30.5165	1.4765	0.3691	11.0739	0.7382
Hum-15	90	12.1	120	4.5	24.4133	2.2627	0.5656	33.5311	1.1313
Hum-16	90	12.1	120	4.5	30.5165	1.6291	0.4072	13.9126	0.8145
Hum-17	90	12.1	120	4.5	36.6199	1.4955	0.3738	6.7899	0.7477
Hum-18	90	12.1	120	4.5	45.7748	1.0955	0.2738	5.0833	0.5477
Hum-19	84	10.4	104	4.5	30.5166	1.2981	0.3245	7.7887	0.649
Hum-20	84	10.4	122	4.5	30.5166	1.2141	0.3035	7.0421	0.607